Glacial/interglacial ice-stream stability in the Weddell Sea embayment, Antarctica

Glacial/interglacial ice-stream stability in the Weddell Sea embayment, Antarctica

Andrew S. Hein *, Christopher J. Fogwill, David E. Sugden and Sheng Xu

*Corresponding Author

School of Geosciences
University of Edinburgh
Drummond Street
Edinburgh, UK
EH8 9XP

Cite As: Hein, AS, Fogwill, CJ, Sugden, DE & Xu, S 2011, 'Glacial/interglacial ice-stream stability in the Weddell Sea embayment, Antarctica' *Earth and Planetary Science Letters*, vol 307, no. 1-2, pp. 211-221.

DOI: 10.1016/j.epsl.2011.04.037

Glacial/interglacial ice-stream stability in the Weddell Sea embayment, Antarctica

Andrew S. Hein[1], Christopher J. Fogwill[2], David E. Sugden[1], Sheng Xu[3]

[1]*School of GeoSciences, University of Edinburgh, Drummond Street, Edinburgh, EH8 9XP, UK.*

[2]*School of Geography, University of Exeter, Streatham Campus, Northcote House, Exeter, EX4 4QJ, UK.*

[3]*Scottish Universities Environmental Research Centre, Rankine Avenue, East Kilbride, G75 0QF, UK.*

Keywords: Antarctic Ice Sheet; dynamic; stable; cosmogenic nuclide surface exposure age dating; Last Glacial Maximum; Miocene.

Abstract

The resilience of the Antarctic Ice Sheet and its effect on global sea level depends on the dynamics of ice streams. Antarctic ice streams are known to be responsive to changes at the ocean interface and, as expected, most have thinned in response to ocean warming and sea-level rise since the Last Glacial Maximum (LGM). Here we provide direct and unexpected evidence that points toward the

glacial/interglacial stability of the Slessor and Recovery glaciers, ice streams of the East Antarctic Ice Sheet (EAIS) which merge with the West Antarctic Ice Sheet (WAIS) to form the Filchner Ice Shelf in the Weddell Sea embayment. Cosmogenic-nuclide measurements in the Shackleton Range seem to suggest that the Slessor and Recovery ice streams were not significantly thicker than today during the LGM. We hypothesise that the glaciers did not thicken because the grounding line was not able to migrate seaward beyond the deep Thiel/Crary Trough beneath the Filchner Ice Shelf immediately offshore. This discovery reveals how a topographic threshold of stability can affect the dynamics of ice streams. It also reduces uncertainties on the thickness, extent and volume of the Antarctic Ice Sheet in a large but unknown sector of the Antarctic Ice Sheet; it constrains the potential sea-level rise from Antarctica; it helps explain observed anomalies in glacio-isostatic adjustment; above all it suggests that the behaviour of the Atlantic-facing Weddell Sea sector of the WAIS contrasts with that of the Pacific-facing Ross and Amundsen Sea sectors.

1. Introduction

Ice streams are linear zones of fast-flowing ice with velocities of hundreds of metres per year. They have low surface gradients because of enhanced sliding at their base and may be tens of km across with crevasses marking clear margins. In many cases the lower reaches of an ice stream may flow through an upland margin and, where they are bounded by rock walls, they are known as outlet glaciers (Sugden, 2009). Ice streams are important because they drain the bulk of ice from Antarctica. Most ice streams in Antarctica lead into floating ice-shelves, which have relatively

flat surfaces and thin from over 1000 m at their inner margins to 100-200 m at the seaward edge where calving of icebergs occurs periodically. The Ross Ice Shelf fringing the Ross Sea and the Filchner-Ronne Ice Shelf bordering the Weddell Sea are the size of large European countries. The behaviour of ice shelves is influenced by the interface with the sea, both in terms of relative sea level and ocean temperatures which can influence the rate of calving. If, for example, sea level falls, ice shelves may become grounded and in such a case they thicken until the surface gradient is sufficient to overcome the increase in basal friction and maintain flow to the sea. In such a case the ice streams flowing into the ice shelf also thicken to maintain their flow.

Throughout Antarctica, onshore and offshore evidence indicates that ice streams and their rock-bounded seaward equivalents, outlet glaciers, expanded and thickened during the LGM (Fig. 1, inset). This is evident around the margins of East Antarctica, including the Lambert Basin (Fink et al., 2006), Mac Robertson Land (Mackintosh et al., 2007), the Transantarctic Mountains in the Ross Sea embayment (Denton and Hughes, 2000 and references therein), and throughout West Antarctica including the Antarctic Peninsula (Bentley et al., 2006), the Weddell Sea (Bentley et al., 2010), the Amundsen Sea (Ackert et al., 1999; Anderson, 1999) and Marie Byrd Land (Stone et al., 2003). Most of the LGM increase in ice volume in Antarctica came from the marine-based WAIS, which nearly doubled in size as it expanded across shelf areas with lowering of eustatic sea level (Denton and Hughes, 2002). In the Ross Sea sector, a number of independent records indicate the WAIS expanded and thickened and was grounded near to the continental shelf edge (Anderson, 1999; Denton and Hughes, 2000; Shipp et al., 1999), and then steadily thinned and retreated throughout

the Holocene (Conway et al., 1999; Stone et al., 2003). Several outlet glaciers that drain the EAIS through the Transantarctic Mountains thickened by 300 – 1000 m in their lower reaches where they joined the expanded WAIS, despite climatic hyper-aridity and potential thinning in source areas on the polar plateau (Bromley et al., 2010; Denton et al., 1989; Ritz et al., 2001; Todd et al., 2010). The dynamics of these East Antarctic outlet glaciers depends more on the location of the grounding line in the Ross Sea than on changes in climate.

The thickness of the LGM ice sheet in the Weddell Sea sector is unknown (Bentley, 1999). Some numerical models and field-based reconstructions produce a thick ice sheet grounded at or near the continental shelf edge, which implies a marked increase in ice volume in the Weddell Sea sector (Bentley, 1999; Denton and Hughes, 2002; Huybrechts, 2002; Pollard and DeConto, 2009; Ritz et al., 2001). Offshore, where the glacially eroded Crary Trough reaches the continental shelf edge, there is a large depocenter for glacigenic sediments, the Crary Fan. The Crary Fan is 3-km thick and seismic-stratigraphy linked to bore-hole chronologies indicates it has been built since the early Miocene (Kuvaas and Kristoffersen, 1991). The presence of the fan and its size supports reconstructions that place the grounding line at or near the continental shelf edge. In contrast, radiocarbon ages of 26 ka on ice-rafted-debris near the shelf-edge in the eastern Weddell Sea indicate the grounding line had retreated landward sometime before the LGM (Anderson and Andrews, 1999).

Onshore, there exists similar uncertainty on the thickness of the LGM ice sheet. Ice thicknesses up to 1900 m higher than the present ice sheet surface have been inferred from well-preserved but poorly dated geologic features such as glacier trimlines, striations and moraines on ice free massifs (Bentley, 1999; Denton and Hughes, 2002; Höfle and Buggisch, 1995; Kerr and Hermichen, 1999). Recent direct dating of some of these glacial features and erratics by cosmogenic-nuclide methods indicate the ice sheet thickened during the LGM but by only 230 – 480 m in the Ellsworth Mountains to the southwest, where steady thinning began by 15 ka (Bentley et al., 2010); furthermore, these results indicate that the higher trimlines in the Ellsworth Mountains are older than the LGM. On the Antarctic Peninsula, the ice may have covered mountain summits, but the ice surface near the Behrendt Mountains on the southern peninsula had lowered to < 300 m above the modern level by 7.2 ka (Bentley et al., 2006). Another constraint on ice thickness comes from oxygen isotope data from the Berkner Island ice core, which suggests that the island was not over-ridden by the WAIS during the LGM (Mulvaney et al., 2005). Finally, recent geodetic measurements of vertical crustal motion suggest that models of glacio-isostatic adjustment are overestimating uplift across much of West Antarctica, implying possible errors in the ice history models (Bevis et al., 2009). Against this background of uncertainty, we provide new geologic data on the thickness of the ice sheet and the Filchner Ice Shelf during the last glacial cycle.

2. The Shackleton Range

The Shackleton Range overlooks the Filchner Ice Shelf to the west and is bounded by two large and fast-flowing ice streams draining the EAIS, the Slessor and Recovery glaciers, which together contribute 80% of the inflow to the Filchner Ice

Shelf (Gray et al., 2001; Jezek et al., 2009) (Fig. 1). Because the Filchner Ice Shelf results from the confluence of both the EAIS and the WAIS, the location provides insight into the history of both ice sheets. To determine the late Pleistocene history of the ice sheet we dated past changes in the thickness of the Slessor Glacier by analysis of in situ produced cosmogenic ^{10}Be and ^{26}Al in glacial sediment and bedrock on the flanks of three presently ice-free mountains, namely, Mt. Provender, Mt. Skidmore and Mt. Sheffield (Fig. 2). These sites were chosen because they are the closest to the main flow of the Slessor Glacier and they span locations both near to and far from its grounding line. Their geology, glacial geomorphology and sediments have been described by Höfle and Buggisch (1995) and Skidmore and Clarkson (1972).

Mt. Provender is located in the northwest of the range where the local Blaiklock and Stratton Glaciers merge with the surface of the Slessor Glacier. The main shear zone at the margin of the Slessor Glacier is situated 15 km NNW of Mt. Provender at an elevation of c. 120 m (RAMP 200m DEM; Liu et al., 2001). Mt Provender has the additional advantage that it is a similar distance from the fast-flowing margin of Recovery Glacier which is at a similar elevation (Fig. 2). Nostok Lake (205 m) sits at the base of Mt. Provender where the local glaciers merge (Figs. 3 and 4). Höfle and Buggisch (1995) identified lodgement till with clasts oriented NNW-SSE at the top of a NW-SE trending scarp 100 m above Nostok Lake and suggested that the Blaiklock Glacier was once higher at this location. Furthermore, they identified little-weathered sandstone erratics that occur at elevations up to 350 m above the modern ice surface and concluded that they represented the limits of the thickening of the Slessor Glacier during the LGM (Fogwill et al., 2004; Höfle and Buggisch, 1995).

Mt. Skidmore is located 20 km northeast of Mt. Provender where the Stratton and Köppen glaciers merge with the Slessor Glacier. The main shear zone of the Slessor Glacier is situated 12 km NNW of Mt. Skidmore at an elevation of c. 180 m (RAMP 200m DEM; Liu et al., 2001). Mt. Skidmore is characterized by low-angled, till-covered slopes with polygons and little exposed bedrock (Fig. 5). Höfle and Buggisch (1995) describe a weathering break at 200 m above the ice surface which they infer to mark the upper limit of the Slessor Glacier during the LGM; this weathering break was observed during our field visit (Fig. 3). Below this level the moraines on the NE shoulder and till are comparatively less weathered. However, the sediments are often iron stained and no striated or typical "fresh" clasts were found. Boulders are generally sparse and poorly preserved with some having disintegrated in situ.

The third site, Mt. Sheffield, is situated on the main shear zone of the Slessor Glacier at an elevation of c. 310 m and 60 km upstream of Mt. Skidmore. Clear and well-preserved moraine ridges are present at elevations of up to 165 m above the modern ice margin (Fig. 6). A dark-coloured drift is evident up to 120 m above the present ice margin and, in common with the other sites, we expected this to mark the height of the Slessor Glacier during and following the LGM. The assumed LGM limits at the three sites imply the greatest thickening at the mouth of the Slessor Glacier and less towards the head in a similar fashion to East Antarctic glaciers flowing into the Ross Sea.

3. Approach and methodology

To determine the late Pleistocene thinning history of the Slessor Glacier, we obtained cosmogenic ^{10}Be and ^{26}Al surface exposure ages from erratic cobbles and occasional bedrock surfaces on the northern flanks of Mt. Provender, Mt. Skidmore and Mt. Sheffield. In principle the approach allows us to track the lowering of the ice sheet surface through time by determining when glacially transported rocks were deposited on the emerging mountain side. This is achieved by measuring the abundance of rare cosmogenic nuclides such as ^{10}Be that form at a known rate through the interaction of cosmic radiation with rock surface minerals. Since the cosmic ray flux attenuates rapidly with depth cosmogenic-nuclides only accumulate within the top few metres of the Earth's surface. Thus analysis of glacier deposits is a way of dating the time a glacier retreated from a mountain side. However, in Antarctica, some glaciers that are frozen to their bed can advance over delicate landforms without disturbing them and the result is a mix of old and young exposure ages in a deposit. In such cases the younger ages are used to constrain the most recent ice thinning (e.g., Ackert et al., 2007; Balco, 2011; Bentley et al., 2006; Bentley et al., 2010; Mackintosh et al., 2007; Stone et al., 2003; Todd et al., 2010).

Our sampling strategy was to collect samples in altitudinal profiles from summits down to the modern ice margins at each site. We preferentially targeted brick-sized erratics with a relatively "fresh" appearance (Figs. 5 and 6). In doing so, we hoped to 1) avoid issues related to sample self-shielding that can occur when a large clast rotates or flips over, and 2) target the youngest samples which should date

the most recent ice thinning. We aimed to identify the highest elevation at which exposure ages date to the last glacial cycle. Such a transition would mark the upper limit of the ice sheet at the time. The specific sample locations are detailed on the aerial photographs in Figure 3 and in Table 1. Photographs of typical samples are shown in Figures 4 – 6. The samples were prepared at the University of Edinburgh's Cosmogenic Nuclide Laboratory (Hein, 2009) and were measured at the AMS facility at the Scottish Universities Environmental Research Centre (Xu et al., 2010).

3.1 Advantages and limitations

The three sites are well-positioned to investigate past elevation changes of the Slessor Glacier, and in one case Recovery Glacier. The Mt. Sheffield site is situated directly on a marginal shear zone and is a direct fix on the elevation of the Slessor Glacier itself. Mt. Skidmore and Mt. Provender are bounded by local glaciers that merge with the Slessor and Recovery glaciers (Fig. 2). Since shear stress at the bed of a glacier is related to ice thickness and surface slope, thickening of the ice streams would be met with concomitant thickening of these local glaciers in response to the reduction in their surface gradients. In this study we make the assumption that the balance of flow remains relatively constant between these local glaciers and the ice streams. Therefore, we assume ice elevation changes on Mt. Provender and Mt. Skidmore reflect changes in the elevation of the Slessor Glacier, while Mt Provender also reflects changes in the Recovery Glacier. It is worth noting that even if the balance shifted to such an extreme that no local glaciers existed at all during the

LGM, the maximum uncertainty this assumption could introduce is an underestimation of thickening by c. 100 m; this value is based on the difference in elevation of our lowest sample at these two sites and the adjacent elevation of the Slessor Glacier.

The altitude profile technique is a common and effective way to determine ice elevation changes in glaciated regions but it also has limitations. The approach we use is partly based on 'negative evidence'. In other words, our upper limit will be defined by the lack of exposure ages dating to the last glacial cycle. As a result, we can never rule out the possibility that clasts dating to the last glacial cycle exist at elevations higher than our upper limit. In an effort to reduce this unavoidable uncertainty we have developed one of the densest cosmogenic-nuclide datasets to sample a single outlet glacier in Antarctica.

4. Results

The cosmogenic-nuclide results are presented in Figures 3 and 7; the data are available in Tables 1 and 2. The exposure ages were calculated using version 2.2 of the CRONUS-Earth exposure age calculator (main calculator v.2.1; constants v.2.2.1; muons v.1.1)(Balco et al., 2008) which implements the recently revised ^{10}Be half-life of 1.387 Ma (Chmeleff et al., 2010; Korschinek et al., 2010). Ages are reported based on the Dunai (2001) scaling model; these differ by up to 6 - 8% depending on the choice of alternative scaling models (Desilets et al., 2006; Lal, 1991; Lifton et al.,

2005; Stone, 2000). The exposure ages assume no rock surface erosion or snow cover correction and thus are minimum ages.

We obtained 83 ^{10}Be and ^{26}Al surface exposure ages from 70 rock samples; of these 42 were taken from within the presumed LGM ice limits and 28 were taken from above. Figure 7 plots the normalised ^{10}Be and ^{26}Al concentrations and approximate exposure ages versus the elevation above the modern ice margin at each site (cf. Sugden et al., 2005). It also plots the ^{26}Al/^{10}Be ratio normalised to a line defining the erosion saturation end-points such that ratios less than 1 indicate a complex exposure history (Lal, 1991). In this environment, complex exposure may indicate periods of burial under ice. Since ^{26}Al decays about twice as fast as ^{10}Be, such shielding can be detected in the ^{26}Al/^{10}Be ratio if the burial period is long enough (Lal, 1991). In the following discussion we rely on ^{10}Be exposure ages.

In a simple case, one would expect to observe a trend of decreasing exposure ages with elevation resulting from the thinning of the ice sheet through time, as is found elsewhere in Antarctica; this is not observed. Instead, and despite sampling the least-weathered rocks available at each site, we find that just eight samples yield exposure ages that date to the last glacial period; these range from 3.0 to 41 ka. Furthermore, these young dates are found only at the modern ice margins at each site. The remaining samples, all above the present ice margin, range in age from 109 ka to a remarkable 1,637 ka. The ^{26}Al/^{10}Be ratios of the latter indicate both continuous and interrupted surface exposures; the former suggests no significant ice cover while the

latter suggest periods of burial. There are no obvious systematic trends with regard to age, altitude or distance from the ice margin. The cause of this distribution in ages is likely due to a range of processes including differential weathering over long time scales and inheritance of cosmogenic-nuclides from previous exposures. Such complex patterns are common in Antarctica (Ackert et al., 2007; Bentley et al., 2006; Bentley et al., 2010; Mackintosh et al., 2007; Stone et al., 2003; Todd et al., 2010).

5. Discussion

5.1 Elevation of the Slessor Glacier at the LGM

5.1.1 Mt. Provender

At Mt. Provender, striated bedrock on the modern ice margin has an age of 11.5 ka while 10 m further away striated bedrock gives an age of 41 ka (Fig. 4). Erratics give ages of 3 ka, 41 ka, and 142 ka, the latter of which reflects prior exposure. Above this point there is an escarpment and the next exposure ages, all > 340 ka, come from elevations above 600 m.

The concordant bedrock and erratic ages suggest the ice margin lowered to its present elevation at 240 m by 41 ka. This implies that the ice was no thicker than today during the LGM and that there has been very little change since. Alternatively, if the age is influenced by previously accumulated nuclides, the thinning to this position could have occurred later. If such a thickening is represented by the

escarpment above Nostok Lake this would imply thickening of about 100 m at Mt Provender.

5.1.2 Mt. Skidmore

At Mt. Skidmore, the two youngest exposure ages and the only dating to the LGM come from the modern ice margin with ages of 27 ka and 120 ka (Fig. 3). The other three samples on the ice margin give ages of 189 ka, 357 ka and 1016 ka. Above the ice margin 22 samples within presumed LGM limits, including 12 located less than 100 m above the modern ice margin, give exposure ages that range between 151 ka and 1024 ka while 17 exposure ages above this level range between 416 ka and 1637 ka.

The results from the ice margin indicate a high proportion of pre-exposed/recycled clasts at this site; however a key finding is that young ages do occur on the modern ice margin which suggests that the glaciers do deposit fresh clasts. Thus, we would expect to find a proportion of young ages at higher elevations if the glacier had thickened during the LGM, as has been observed elsewhere in Antarctica (Ackert et al., 1999; Bentley et al., 2006; Mackintosh et al., 2007; Stone et al., 2003). Despite sampling the freshest appearing clasts none of the 39 samples that were taken from above the ice margin give ages consistent with the last glacial cycle (circles, Fig. 7). The most obvious explanation for the exposure age results is that the ice margin was no higher than at present during the LGM.

5.1.3 Mt. Sheffield

At Mt. Sheffield the three youngest exposure ages and the only ones dating to the LGM come from the modern ice margin with ages of 3 ka, 23 ka and 25 ka (Fig. 3). A fourth exposure age of 401 ka also on the ice margin reflects pre-exposure despite a seemingly fresh appearance (Fig. 6). Above the ice margin, six samples taken from across the dark drift moraines give ages of 109 ka to 850 ka, and above this, four samples give ages of 267 ka to 822 ka.

The most obvious explanation for the exposure age results is that the ice margin was no higher than at present (310 m) during the LGM. It is difficult to support alternative explanations that assume a thicker ice sheet at the time. Mt. Sheffield is situated on the main shear zone of the Slessor Glacier and there are clear moraine ridges visible. Therefore, we consider it unlikely that this area was covered by cold-based ice and associated non-deposition. Our results from the modern ice margin suggest that the proportion of pre-exposed/recycled clasts is low at this location (1 in 4) and thus it is unlikely that all ten clasts taken from above the ice margin are recycled.

5.1.4 Discussion

The key finding is that 'young' (last glacial cycle) ages are restricted to the modern ice margins at each site and despite sampling many relatively "fresh" clasts from within the presumed LGM limits. The ^{10}Be exposure ages reveal a consistent pattern at all three sites that points to limited change in the elevation of the Slessor and Recovery glaciers during and since the LGM; it points to the glacial/interglacial stability of these major ice streams.

Nevertheless, it is worth exploring alternative explanations. If the ice sheet did thicken during the LGM as it did in most other parts of Antarctica, one possibility is that we simply did not sample the young rocks related to this advance. This scenario seems unlikely given our sampling strategy which aimed to reduce this uncertainty and the sheer number of samples we collected from within the presumed LGM limits. A related possibility is that our sampling strategy of choosing brick-sized clasts is overly biased towards clasts with inheritance; perhaps if we sampled larger boulders we would have got a different result, although few of these exist and most are poorly preserved. A further possibility is that the area was covered by cold-based ice which did not deposit any new material or very little new material on the mountainside. One way this may occur is if there was little or no lateral movement to bring new material to the surface. Since the ice is moving and building a moraine today (Fig. 3) and there exists lateral moraines on, for example, the NE shoulder of Mt. Skidmore, the change in ice dynamics implied by this scenario seems unlikely. Alternatively, there could be lateral movement of debris-poor cold-based ice. It is difficult to entirely rule-out this possibility of non-deposition by cold-based ice; the interpretation requires pervasive prior exposure at this site which may not be detected in ^{26}Al/^{10}Be ratios.

While alternative explanations cannot be ruled-out entirely, they seem to require special conditions that either appear unlikely or do not fit observations. Thus, when considering the overall pattern of ^{10}Be exposure ages observed at all three sites, the most obvious explanation and our favoured interpretation is that there has been little or no change in the elevation of the Slessor and Recovery ice streams since the LGM.

5.2 Ice stream mechanisms

The lack of change of the Slessor and Recovery glaciers is puzzling when considering the well-documented and consistent pattern of LGM thickening and subsequent thinning that occurred in the lower reaches of East Antarctic ice streams and outlet glaciers in the Ross Sea sector. Given the demonstrated link with grounding line fluctuations in the Ross Sea, one would expect a similar response in the Weddell Sea had the ice sheet been grounded as far as the continental shelf edge, c. 800 km distant from Mt. Provender. The switch from a floating ice shelf to a grounded ice stream would cause 1) a rise in basal shear stress, 2) a reduction in ice velocity and 3) thickening. Such thickening would be expected even in the case of a fast-flowing ice stream with low basal traction, as geologic data from the Reedy Glacier and Ohio Range indicate for the Mercer Ice Stream in the Ross Sea sector (see Ackert et al., 2007; Parizek and Alley, 2004; Todd et al., 2010). No such change in the height of the Slessor and Recovery glaciers was observed and since an unfeasibly low surface gradient (c. 0.0003) would otherwise be required to explain this lack of change, we argue the ice was not grounded at the shelf-edge.

The most obvious explanation for the limited change in elevation, therefore, is a constraint on the position of the grounding line in the Weddell Sea. Bathymetry reveals the depth of the Thiel/Crary Trough, located beneath the Filchner Ice Shelf and immediately offshore, is more than 1,400 m below sea level (Makinson and Nicholls, 1999) (Fig. 8). The depth is similar or greater than troughs elsewhere in Antarctica where ice streams were grounded during the LGM, for example, in Marguerite Bay on the west side of the Antarctic Peninsula where ice was grounded at depths of 1000 m (Anderson and Fretwell, 2008). It may simply be that the Filchner Ice Shelf can drain all the ice that the two ice streams deliver and that the glaciers are unable to ground as a result. A factor favouring this scenario is that the ice streams deliver ice to the flanks of the trough in a geometry that is optimal for discharging floating ice. The bathymetry, while coarse in resolution, supports this scenario.; it reveals an east-west trending trough cut by the Slessor and Bailey glaciers entering the deeper Thiel/Crary Trough as a hanging valley (Fig. 8).

In summary, our finding that the Slessor and Recovery glaciers did not thicken more than present during the LGM leads us to suggest the ice was not grounded in the Thiel/Crary Trough north of c. 80º S. The implication is that the Filchner Ice Shelf did not ground and that the ice extent and volume in the Weddell Sea sector of Antarctica cannot have increased significantly during the LGM. Our results and interpretations are consistent with radiocarbon ages that indicate the ice sheet had retreated from the shelf edge prior to the maximum sea-level lowering of the LGM

(Anderson and Andrews, 1999), and with the model results of Bentley *et al.* (2010), who produced a 'thin' LGM ice sheet only by restricting the migration of the grounding line. Furthermore, our finding of stability is consistent with GPS measurements from Whichaway Nunataks, a rock outcrop on the south side of Recovery Glacier, which record current subsidence as opposed to the uplift expected in areas that have experienced postglacial thinning (Bevis et al., 2009). Satellite altimeter and interferometric-radar measurements seem to indicate modern thickening of the Slessor Glacier on decadal timescales (Davis et al., 2005; Joughin and Bamber, 2005) and thus could help explain the current rock subsidence. We suspect the elevated moraine ridges evident at Mt. Sheffield and Mt. Skidmore probably reflect thinning during successive glaciations.

5.3 Wider implications

The Thiel/Crary trough is one of a series of glacial troughs on land and offshore in Antarctica that reflects an expanded ice sheet extending to the outer margin of the continental shelf (Jamieson and Sugden, 2008). Such troughs have characteristics of glacial erosion, such as overdeepened basins, hanging valleys and large meltwater channel systems cut in bedrock. Elsewhere such troughs have been dated to a mid-Miocene expansion at ~ 14 million years ago. For example, Wright Valley in the McMurdo Dry Valleys was cut by an ice sheet that was thicker than that of today. The presence of undisturbed volcanic ash deposits of 14 Ma in the channels of the associated Labyrinth meltwater channel system (Lewis et al., 2006) show that the

trough was cut before or in the mid-Miocene. Such an age is confirmed by an offshore record of ice extending over the Pacific-facing continental shelf in the mid-Miocene before retreating to its current extent around 13.5 Ma (Anderson, 1999) and by recent analysis of sediments in the ANDRILL core in the Ross Sea (Passchier et al., 2011). The largest trough of all, the Lambert trough, is thought to have been overdeepened by 14 Ma in the mid-Miocene, since when it has not been occupied by grounded ice (Taylor et al., 2004). By analogy, the Thiel/Crary Trough, cut by ice extending to the outer edge of the offshore shelf may also have been eroded by the same extended ice sheet at this time.

We hypothesise that following its erosion ~14 Ma the Thiel/Crary trough has played a role in limiting the expansion of the ice sheet in this part of the Weddell Sea. Since the Bailey, Recovery, Support Force and part of the Foundation Ice Stream also followed the Thiel/Crary Trough during the LGM, we predict limited thickening of these glaciers and thus limited change over a major portion of the ice sheet in the Weddell Sea sector. It appears to be an excellent example of self-limiting behaviour by an ice sheet by which glacial erosion erodes in such a way as to change the dynamics of subsequent ice sheets (Jamieson et al., 2010). The net result is that the volume of ice in this part of the Weddell Sea sector during the LGM is less than previously considered and less even than the minimum estimates of Bentley *et al.* (2010).

This discovery of limited thinning of Slessor and Recovery glaciers since the LGM has a number of additional implications. First, our age determinations demonstrate that many fresh glacial features such as moraines and striations, on which past LGM reconstructions were based, are older than their appearance first suggests, probably due to long-term, low erosion rates (Bentley et al., 2006; Bentley et al., 2010; Fogwill et al., 2004). Second, the constraint on LGM ice volumes for this sector of Antarctica implies a minimal contribution to postglacial sea-level-rise and an insufficient ice volume to account for major meltwater pulses such as Meltwater Pulse 1A and is thus in agreement with Bentley et al. (2010). Third, the thin ice sheet at the LGM may help explain some of the mismatch observed between models of glacio-isostatic adjustment and recent GPS measurements of vertical crustal motion (Bevis et al., 2009) and thus permit improved estimates of glacio-isostatic adjustment that are critical to correct satellite measurements of contemporary ice mass changes in Antarctica. Finally, this study demonstrates the value of geologic data in constraining the past configuration of the ice sheet and its trajectory of change; in this case the Atlantic-facing Weddell Sea sector of the WAIS has responded to climate and sea-level change in a different way compared to the Pacific-facing Ross and Amundsen Sea sectors.

6. Conclusions:

- In the Shackleton Range, cosmogenic ^{10}Be and ^{26}Al surface exposure ages that date to the last glacial cycle were found only at the modern ice margins on Mt. Provender, Mt. Skidmore and Mt. Sheffield.

- The lack of such last-glacial-cycle ages above the Slessor Glacier suggests that it and Recovery Glacier were not significantly thicker than today during the LGM.

- The reason for this, we hypothesise, is because ice could not ground in the Thiel/Crary Trough beneath the Filchner Ice Shelf immediately offshore; north of c. 80º S. Such a grounding-line constraint would also affect the Bailey, Recovery, Support Force and part of the Foundation Ice Streams. Thus we predict limited or modest LGM ice elevation change across a major portion of the Weddell Sea sector of the Antarctic Ice Sheet.

- This is an example of self limiting behaviour by which an ice sheet creates a topographic threshold of stability that goes on to change subsequent ice stream dynamics.

7. Acknowledgements

We thank the UK Natural Environment Research Council (NERC) and the Scottish Alliance for Geoscience, Environment and Society (SAGES); Antarctic Logistics and Expeditions (ALE) for logistical support; I. Joughin for supplying ice-velocity data; A. Le Brocq for bathymetry; and E. McDougall for laboratory support. We are grateful for the constructive comments of two anonymous reviewers which helped to improve this manuscript.

8. References

Ackert, R.P., Barclay, D.J., Borns, H.W., Calkin, P.E., Kurz, M.D., Fastook, J.L., and Steig, E.J., 1999, Measurements of past ice sheet elevations in interior West Antarctica: Science, v. 286, p. 276-280.

Ackert, R.P., Mukhopadhyay, S., Parizek, B.R., and Borns, H.W., 2007, Ice elevation near the West Antarctic Ice Sheet divide during the Last Glaciation: Geophysical Research Letters, v. 34.

Anderson, J.B., 1999, Antarctic marine geology: Cambridge, Cambridge University Press.

Anderson, J.B., and Andrews, J.T., 1999, Radiocarbon constraints on ice sheet advance and retreat in the Weddell Sea, Antarctica: Geology, v. 27, p. 179-182.

Anderson, J.B., and Fretwell, U.O., 2008, Geomorphology of the onset area of a paleo-ice stream, Marguerite Bay, Antarctic Peninsula: Earth Surface Processes And Landforms, v. 33, p. 503-512.

Balco, G., 2011, Contributions and unrealized potential contributions of cosmogenic-nuclide exposure dating to glacier chronology, 1990-2010: Quaternary Science Reviews, v. 30, p. 3-27.

Balco, G., Stone, J.O., Lifton, N.A., and Dunai, T.J., 2008, A complete and easily accessible means of calculating surface exposure ages or erosion rates from Be-10 and Al-26 measurements: Quaternary Geochronology, v. 3, p. 174-195.

Bentley, M.J., 1999, Volume of Antarctic Ice at the Last Glacial Maximum, and its impact on global sea level change: Quaternary Science Reviews, v. 18, p. 1569-1595.

Bentley, M.J., Fogwill, C.J., Kubik, P.W., and Sugden, D.E., 2006, Geomorphological evidence and cosmogenic Be-10/Al-26 exposure ages for the Last Glacial Maximum

and deglaciation of the Antarctic Peninsula Ice Sheet: Geological Society Of America Bulletin, v. 118, p. 1149-1159.

Bentley, M.J., Fogwill, C.J., Le Brocq, A.M., Hubbard, A.L., Sugden, D.E., Dunai, T.J., and Freeman, S., 2010, Deglacial history of the West Antarctic Ice Sheet in the Weddell Sea embayment: Constraints on past ice volume change: Geology, v. 38, p. 411-414.

Bevis, M., Kendrick, E., Smalley, R., Dalziel, I., Caccamise, D., Sasgen, I., Helsen, M., Taylor, F.W., Zhou, H., Brown, A., Raleigh, D., Willis, M., Wilson, T., and Konfal, S., 2009, Geodetic measurements of vertical crustal velocity in West Antarctica and the implications for ice mass balance: Geochemistry Geophysics Geosystems, v. 10.

Bierman, P.R., Caffee, M.W., Davis, P.T., Marsella, K., Pavich, M., Colgan, P., Mickelson, D., and Larsen, J., 2002, Rates and timing of earth surface processes from in situ-produced cosmogenic Be-10, Beryllium: Mineralogy, Petrology, And Geochemistry, Volume 50: Reviews In Mineralogy & Geochemistry: Washington, Mineralogical Soc America, p. 147-205.

Bromley, G.R.M., Hall, B.L., Stone, J.O., Conway, H., and Todd, C.E., 2010, Late Cenozoic deposits at Reedy Glacier, Transantarctic Mountains: implications for former thickness of the West Antarctic Ice Sheet: Quaternary Science Reviews, v. 29, p. 384-398.

Chmeleff, J., von Blanckenburg, F., Kossert, K., and Jakob, D., 2010, Determination of the Be-10 half-life by multicollector ICP-MS and liquid scintillation counting: Nuclear Instruments & Methods in Physics Research Section B-Beam Interactions with Materials and Atoms, v. 268, p. 192-199.

Conway, H., Hall, B.L., Denton, G.H., Gades, A.M., and Waddington, E.D., 1999, Past and future grounding-line retreat of the West Antarctic Ice Sheet: Science, v. 286, p. 280-283.

Davis, C.H., Li, Y.H., McConnell, J.R., Frey, M.M., and Hanna, E., 2005, Snowfall-driven growth in East Antarctic ice sheet mitigates recent sea-level rise: Science, v. 308, p. 1898-1901.

Denton, G.H., Bockheim, J.G., Wilson, S.C., and Stuiver, M., 1989, Late Wisconsin and early Holocene glacial history, inner Ross embayment, Antarctica: Quaternary Research, v. 31, p. 151-182.

Denton, G.H., and Hughes, T.J., 2000, Reconstruction of the Ross ice drainage system, Antarctica, at the last glacial maximum: Geografiska Annaler Series A-Physical Geography, v. 82A, p. 143-166.

—, 2002, Reconstructing the Antarctic Ice Sheet at the Last Glacial Maximum: Quaternary Science Reviews, v. 21, p. 193-202.

Desilets, D., Zreda, M., and Prabu, T., 2006, Extended scaling factors for in situ cosmogenic nuclides: New measurements at low latitude: Earth and Planetary Science Letters, v. 246, p. 265-276.

Dunai, T.J., 2001, Influence of secular variation of the geomagnetic field on production rates of in situ produced cosmogenic nuclides: Earth and Planetary Science Letters, v. 193, p. 197-212.

Fink, D., McKelvey, B., Hambrey, M.J., Fabel, D., and Brown, R., 2006, Pleistocene deglaciation chronology of the Amery Oasis and Radok Lake, northern Prince Charles Mountains, Antarctica: Earth And Planetary Science Letters, v. 243, p. 229-243.

Fogwill, C.J., Bentley, M.J., Sugden, D.E., Kerr, A.R., and Kubik, P.W., 2004, Cosmogenic nuclides Be-10 and Al-26 imply limited Antarctic Ice Sheet thickening and low erosion in the Shackleton Range for > 1 m.y: Geology, v. 32, p. 265-268.

Gray, A.L., Short, N., Mattar, K.E., and Jezek, K.C., 2001, Velocities and flux of the Filchner ice shelf and its tributaries determined from speckle tracking interferometry: Canadian Journal of Remote Sensing, v. 27, p. 193-206.

Haran, T., Bohlander, J., Scambos, T., Painter, T., and Fahnestock, M., 2005, updated 2006, MODIS mosaic of Antarctica (MOA) image map. Boulder, Colorado USA: National Snow and Ice Data Center. Digital Media.

Hein, A.S., 2009, Quaternary Glaciations in the Lago Pueyrredón Valley, Argentina [PhD thesis]: Edinburgh, University of Edinburgh.

Höfle, H.-C., and Buggisch, W., 1995, Glacial Geology and Petrography of Erratics in the Shackleton Range, Antarctica: Polarforschung, v. 63, p. 183-201.

Huybrechts, P., 2002, Sea-level changes at the LGM from ice-dynamic reconstructions of the Greenland and Antarctic ice sheets during the glacial cycles: Quaternary Science Reviews, v. 21, p. 203-231.

Ivy-Ochs, S., 1996, The dating of rock surfaces using in situ produced ^{10}Be, ^{26}Al and ^{36}Cl, with examples from Antarctica and the Swiss Alps: ETH Zurich, unpublished PhD thesis.

Jezek, K., Floricioiu, D., Farness, K., Yague-Martinez, N., and Eineder, M., 2009, TerraSAR-X observations of the recovery glacier system, Antarctica, Geoscience and Remote Sensing Symposium,2009 IEEE International,IGARSS 2009, Volume 2, p. II-226-II-229.

Jezek, K., and Team, R.P., 2002 RAMP AMM-1 SAR Image Mosaic of Antarctica, Fairbanks, AK: Alaska SAR Facility, in association with the National Snow and Ice Data Center, Boulder, CO. Digital media.

Joughin, I., and Bamber, J.L., 2005, Thickening of the ice stream catchments feeding the Filchner-Ronne Ice Shelf, Antarctica: Geophysical Research Letters, v. 32, p. 4.

Kerr, A., and Hermichen, W.D., 1999, Glacial modification of the Shackleton Range, Antarctica: Terra Antarctica, v. 6, p. 353-360.

Kohl, C.P., and Nishiizumi, K., 1992, Chemical Isolation of Quartz for Measurement of Insitu-Produced Cosmogenic Nuclides: Geochimica et Cosmochimica Acta, v. 56, p. 3583-3587.

Korschinek, G., Bergmaier, A., Faestermann, T., Gerstmann, U.C., Knie, K., Rugel, G., Wallner, A., Dillmann, I., Dollinger, G., von Gostomski, C.L., Kossert, K., Maiti, M., Poutivtsev, M., and Remmert, A., 2010, A new value for the half-life of Be-10 by Heavy-Ion Elastic Recoil Detection and liquid scintillation counting: Nuclear Instruments & Methods in Physics Research Section B-Beam Interactions with Materials and Atoms, v. 268, p. 187-191.

Kuvaas, B., and Kristoffersen, Y., 1991, The Crary Fan - A trough-mouth fan on the Weddell Sea continental-margin, Antarctica: Marine Geology, v. 97, p. 345-362.

Lal, D., 1991, Cosmic-Ray Labeling Of Erosion Surfaces - Insitu Nuclide Production-Rates And Erosion Models: Earth And Planetary Science Letters, v. 104, p. 424-439.

Lifton, N.A., Bieber, J.W., Clem, J.M., Duldig, M.L., Evenson, P., Humble, J.E., and Pyle, R., 2005, Addressing solar modulation and long-term uncertainties in scaling secondary cosmic rays for in situ cosmogenic nuclide applications: Earth and Planetary Science Letters, v. 239, p. 140-161.

Liu, H., Jezek, K., Li, B., and Zhao, Z., 2001, Radarsat Antarctic Mapping Project digital elevation model version 2, Boulder, CO: National Snow and Ice Data Center. Digital Media.

Mackintosh, A., White, D., Fink, D., Gore, D.B., Pickard, J., and Fanning, P.C., 2007, Exposure ages from mountain dipsticks in Mac. Robertson Land, East Antarctica, indicate little change in ice-sheet thickness since the Last Glacial Maximum: Geology, v. 35, p. 551-554.

Makinson, K., and Nicholls, K.W., 1999, Modeling tidal currents beneath Filchner-Ronne Ice Shelf and on the adjacent continental shelf: their effect on mixing and transport: Journal of Geophysical Research-Oceans, v. 104, p. 13449-13465.

Mulvaney, R., Arrowsmith, C., Roberts, S., Hillenbrand, C., Hodgson, D., and Barnola, J., 2005, Evidence that Berkner Island, Antarctica, was not over-ridden during the Last Glacial Maximum, American Geophysical Union - Fall Meeting: San Francisco, CA.

Nishiizumi, K., 2004, Preparation of Al-26 AMS standards: Nuclear Instruments & Methods in Physics Research Section B, v. 223-24, p. 388-392.

Nishiizumi, K., Imamura, M., Caffee, M.W., Southon, J.R., Finkel, R.C., and McAninch, J., 2007, Absolute calibration of Be-10 AMS standards: Nuclear Instruments & Methods in Physics Research Section B, v. 258, p. 403-413.

Parizek, B.R., and Alley, R.B., 2004, Ice thickness and isostatic imbalances in the Ross Embayment, West Antarctica: model results: Global And Planetary Change, v. 42, p. 265-278.

Pollard, D., and DeConto, R.M., 2009, Modelling West Antarctic ice sheet growth and collapse through the past five million years: Nature, v. 458, p. 329-U89.

Ritz, C., Rommelaere, V., and Dumas, C., 2001, Modeling the evolution of Antarctic ice sheet over the last 420,000 years: Implications for altitude changes in the Vostok region: Journal of Geophysical Research-Atmospheres, v. 106, p. 31943-31964.

Shipp, S., Anderson, J., and Domack, E., 1999, Late Pleistocene-Holocene retreat of the West Antarctic Ice-Sheet system in the Ross Sea: Part 1 - Geophysical results: Geological Society Of America Bulletin, v. 111, p. 1486-1516.

Skidmore, M.J., and Clarkson, P.D., 1972, Physiography and Glacial Geomorphology of the Shackleton Range: British Antarctic Survey Bulletin, v. 30, p. 69-80.

Stone, J.O., 2000, Air pressure and cosmogenic isotope production: Journal Of Geophysical Research-Solid Earth, v. 105, p. 23753-23759.

Stone, J.O., Balco, G.A., Sugden, D.E., Caffee, M.W., Sass, L.C., Cowdery, S.G., and Siddoway, C., 2003, Holocene deglaciation of Marie Byrd Land, West Antarctica: Science, v. 299, p. 99-102.

Sugden, D.E., 2009, Ice sheets and ice caps, *in* Slaymaker, O., Spencer, T., and Embleton-Hamann, C., eds., Geomorphology and Global Environmental Change: Cambridge, Cambridge University Press, p. 368-402.

Sugden, D.E., Balco, G., Cowdery, S.G., Stone, J.O., and Sass, L.C., 2005, Selective glacial erosion and weathering zones in the coastal mountains of Marie Byrd Land, Antarctica: Geomorphology, v. 67, p. 317-334.

Todd, C., Stone, J., Conway, H., Hall, B., and Bromley, G., 2010, Late Quaternary evolution of Reedy Glacier, Antarctica: Quaternary Science Reviews, v. 29, p. 1328-1341.

Xu, S., Dougans, A.B., Freeman, S., Schnabel, C., and Wilcken, K.M., 2010, Improved Be-10 and Al-26-AMS with a 5 MV spectrometer: Nuclear Instruments & Methods in Physics Research Section B-Beam Interactions with Materials and Atoms, v. 268, p. 736-738.

Figure captions

Figure 1. Location of study area

The inset map of Antarctica shows the location of sites discussed in the text. The main figure is a map of the eastern Weddell Sea showing ice velocities for three major ice streams feeding the Filchner Ice Shelf; warm colours indicate fast flow-rates of up to 1,500 m a^{-1} (red), reducing to < 100 m a^{-1} (green) as illustrated by the progressively

cooler colours (after Joughin and Bamber, 2005). The sample locations in the Shackleton Range are circled. Grounding the Filchner Ice Shelf would cause a reduction in its velocity and backing-up (thickening) of the inflowing ice streams, however, no such change of the Slessor ice stream is evident during the LGM period, which suggests that the ice shelf was not grounded at this time. The base map is the MODIS Mosaic of Antarctica image map (Haran et al., 2005, updated 2006).

Figure 2. The Shackleton Range

A radar image of the Shackleton Range showing the three sites investigated and their relationship to local glaciers and the main shear zone of the Slessor Glacier. We assume the balance of flow during the LGM would remain similar and thus the glaciers would rise and fall together. Image: RAMP AMM-1 SAR Image Mosaic of Antarctica (Jezek and Team, 2002).

Figure 3. Sample locations.

Aerial photographs showing ^{10}Be exposure ages of samples collected at the locations shown on a) Mt. Skidmore, b) Mt. Provender and c) Mt. Sheffield. The dashed line in (a) is the weathering break identified by Höfle and Buggisch (1995) where relatively unweathered surfaces are found to the north of this line. The dashed line in (b) is a scarp 100 m above Nostok Lake. The youngest exposure ages and the only exposure ages dating to the last glacial cycle are found at the modern ice margins at each site. (Source: Alfred Wegener Institute).

Figure 4. Mt. Provender samples.

The photograph shows the location where bedrock and erratic exposure ages were obtained at the ice margin. The inset photograph shows an erratic boulder perched on bedrock near the summit of Mt. Provender at 893 m. The exposure ages suggest that this boulder has survived on the summit for at least 680 ka.

Figure 5. Mt. Skidmore samples.

This figure shows four different samples (inset photographs) and their context (A-D). The location of these samples (labelled) can be found in Figure 3. We targeted the freshest appearing brick-sized erratics that could be found but these were often very old.

Figure 6. Mt. Sheffield samples.

Photograph of (A) the dark-coloured moraines on Mt. Sheffield; in contrast to expectations, these are older than the last glacial cycle. Like elsewhere, exposure ages dating to the LGM were only found at the modern ice margin. Two fresh looking samples on the modern ice margin are shown in (B) and (C); despite their unweathered appearances, their ages range between 3 ka to 400 ka, and comprise the youngest and oldest found at this ice marginal location.

Figure 7. Cosmogenic-nuclide results.

Plot of elevation vs. the ^{10}Be and ^{26}Al concentration of each sample normalised to its production rate. Uncertainties are 1σ analytical. The lower scale approximates the ^{10}Be age. The left plot details samples with low nuclide concentrations that equate to Late Pleistocene ages, these young ages occur at the modern ice margin but not above, suggesting the ice sheet did not thicken during the LGM. The right plot shows the ^{26}Al/^{10}Be ratios normalised to a line defining the erosion-saturation end-points. Samples plotting left of 1.0 indicate a complex exposure history, which may have involved periods of post-depositional burial.

Figure 8. Bathymetry map

Bathymetry (Makinson and Nicholls, 1999) of the southern and eastern Weddell Sea showing the Thiel/Crary Trough, which reaches depths exceeding 1,500 m below sea-level beneath the Filchner Ice Shelf (white wavy line) east of Berkner Island. Contour interval 100 m. We hypothesis that this deep trough has played a role in limiting significant seaward migration of the grounding line of the Slessor Glacier; a control that would also affect the Bailey, Recovery, Support Force and Foundation Glaciers. A trough cut by the Bailey and Slessor glaciers can be seen entering the flank of the Thiel/Crary trough as a hanging valley. The base map is the MODIS Mosaic of Antarctica image map (Haran et al., 2005, updated 2006).

Figure 1 - colour on web and in print
Click here to download high resolution image

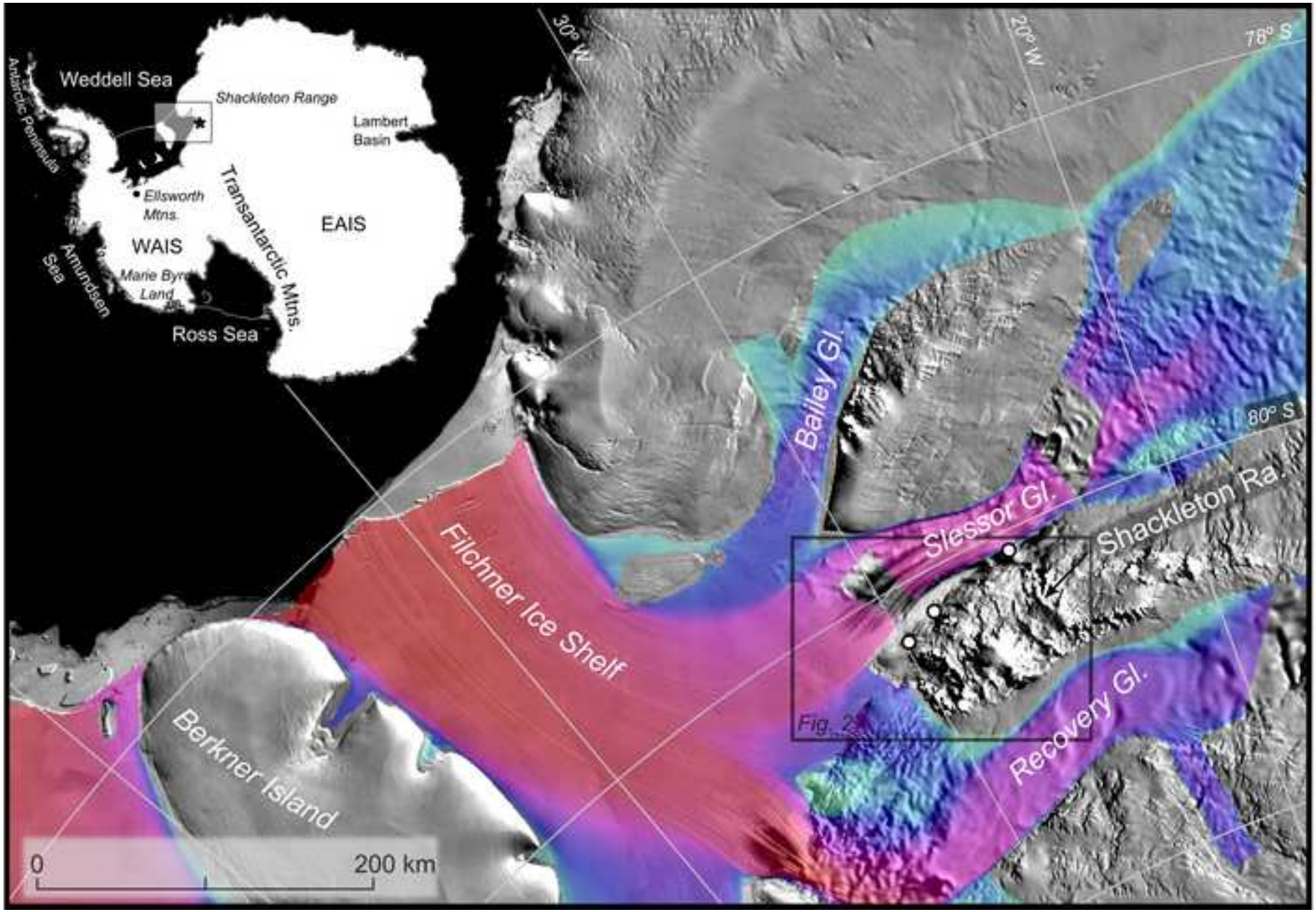

Figure 2

Click here to download high resolution image

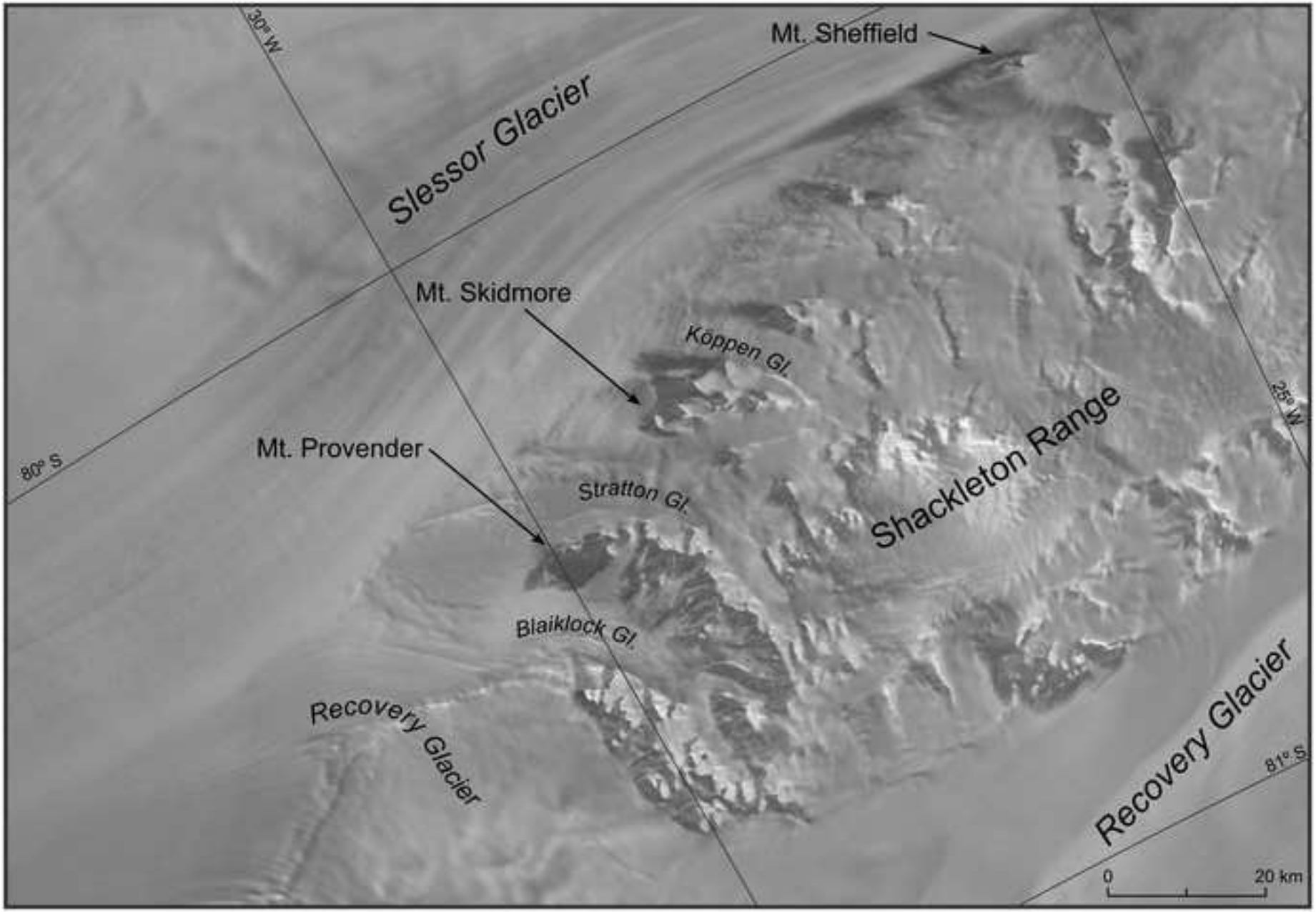

Figure 3

Click here to download high resolution image

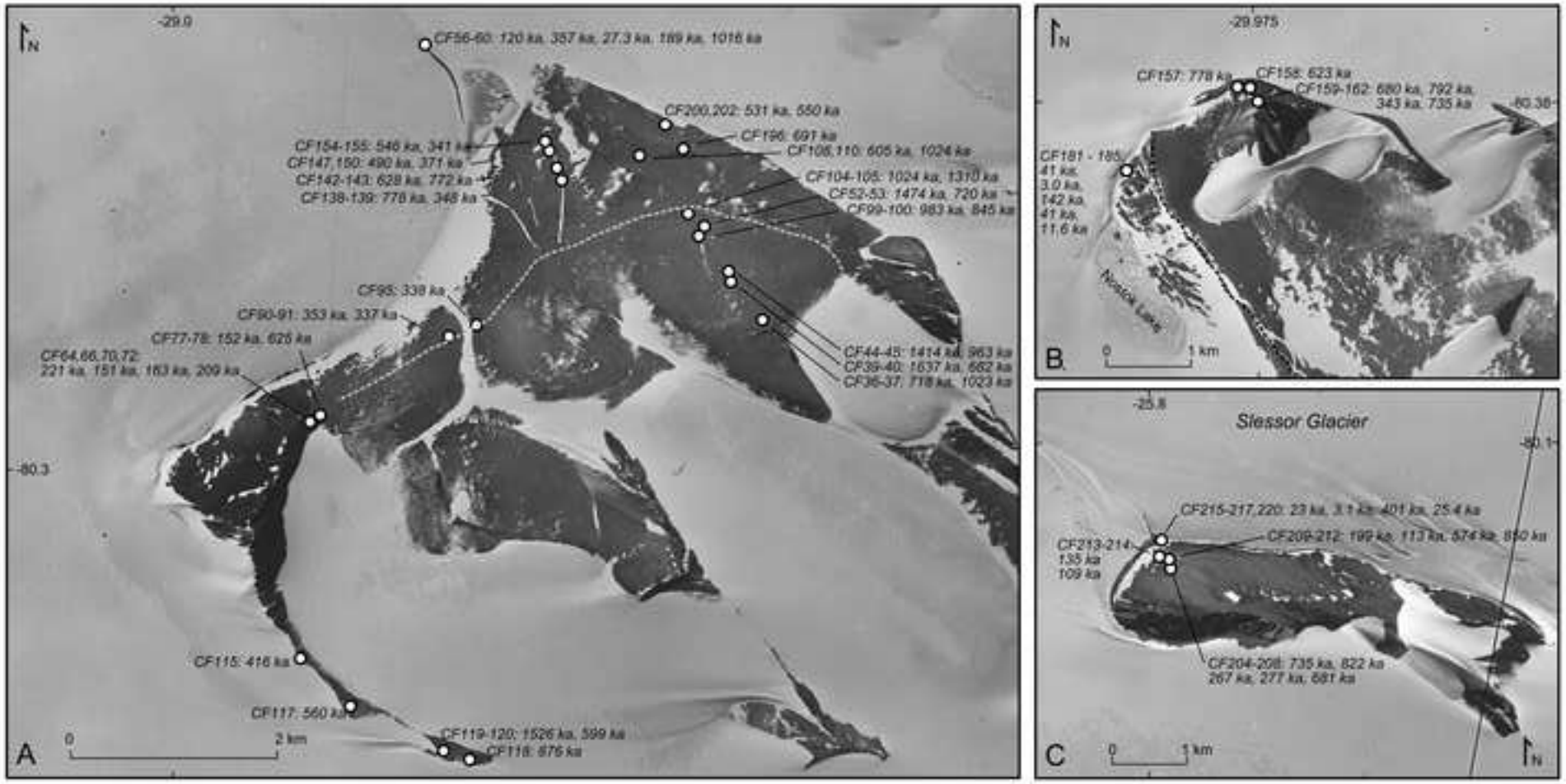

Figure 4 - colour on web only

Click here to download high resolution image

Figure 5 - colour on web only

Click here to download high resolution image

Figure 6 - colour on web only
Click here to download high resolution image

Figure 7

Click here to download high resolution image

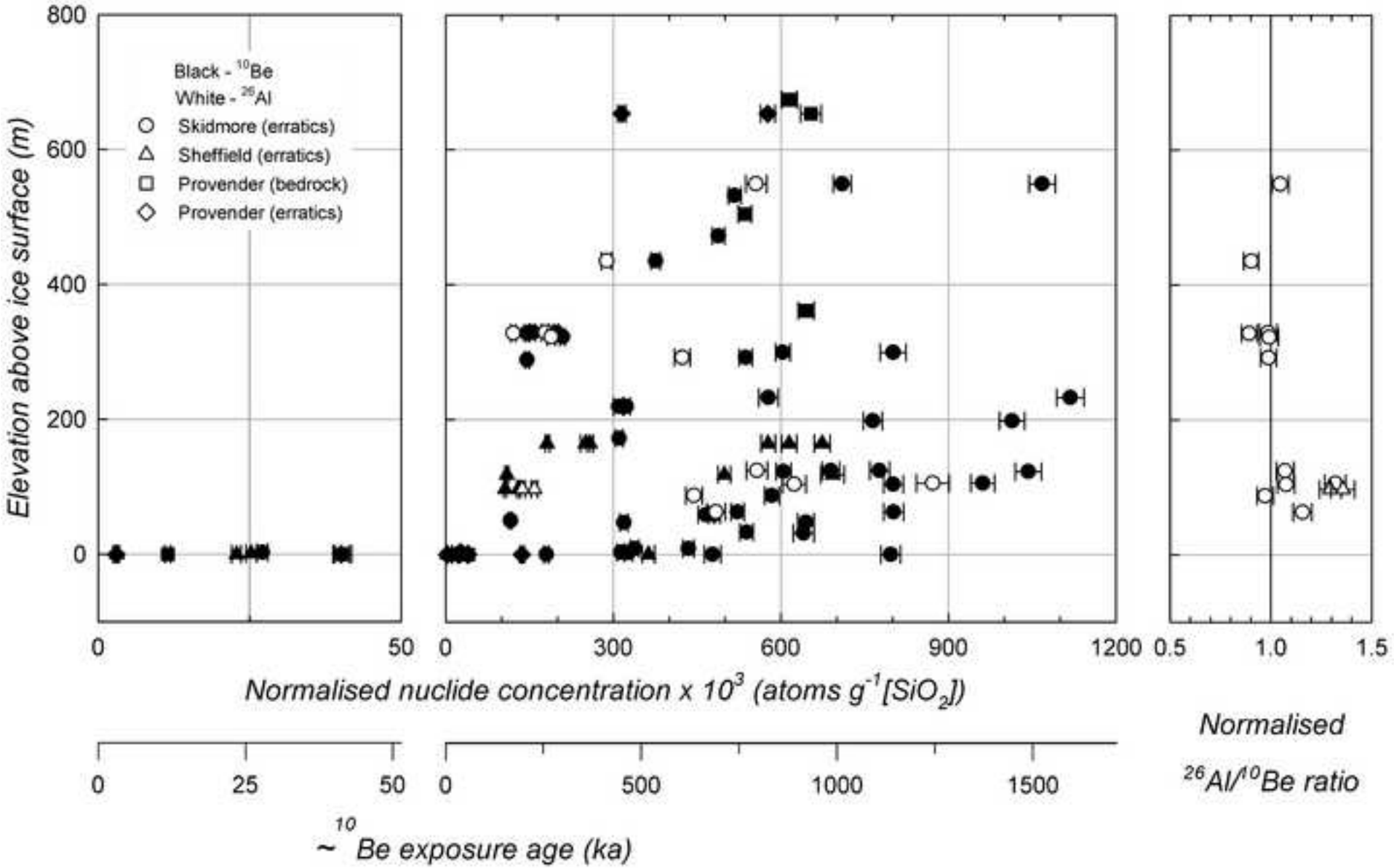

Figure 8 - colour on web and in print
Click here to download high resolution image

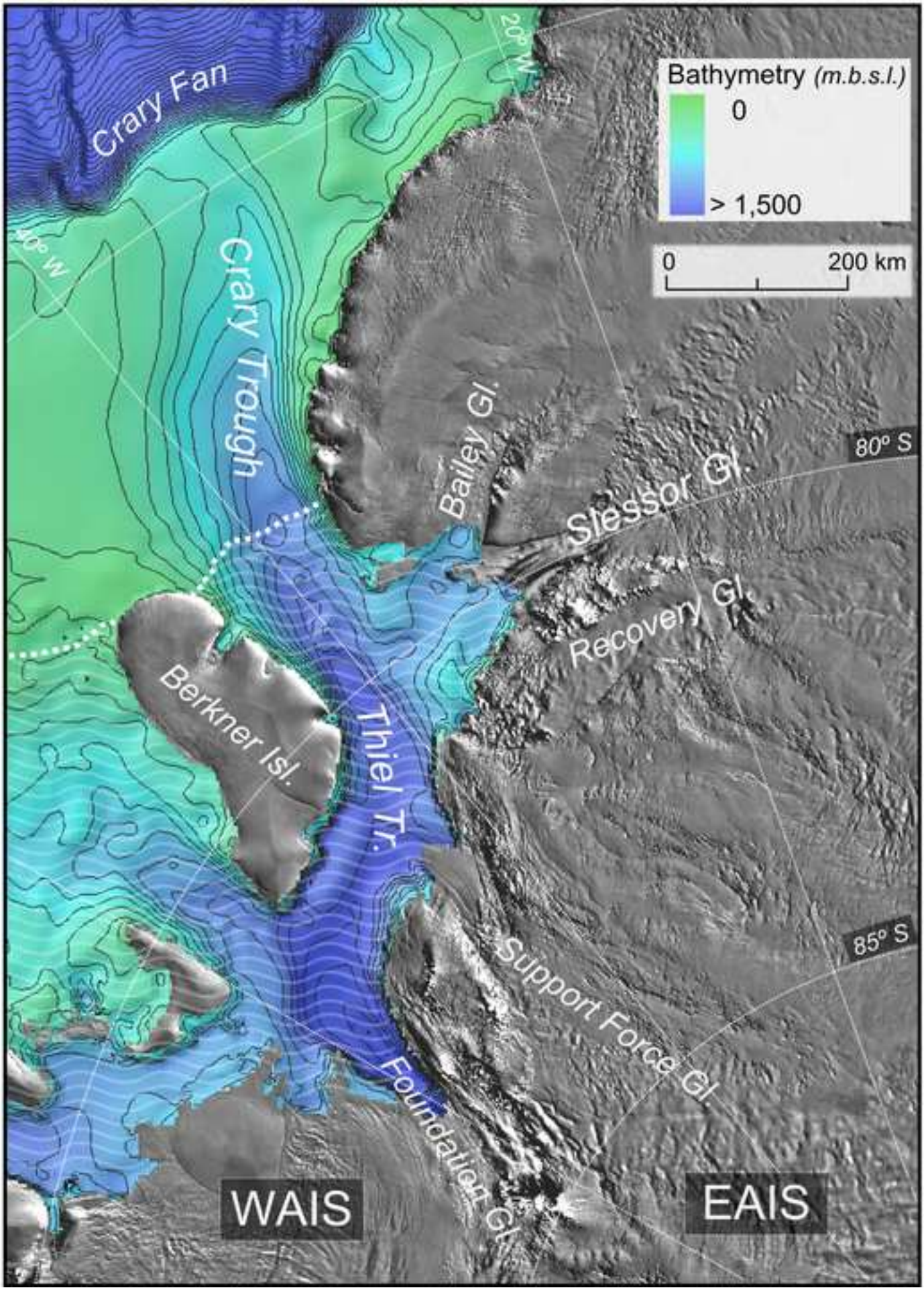

Figure 4 - black and white print version
Click here to download high resolution image

Figure 5 - black and white print version
Click here to download high resolution image

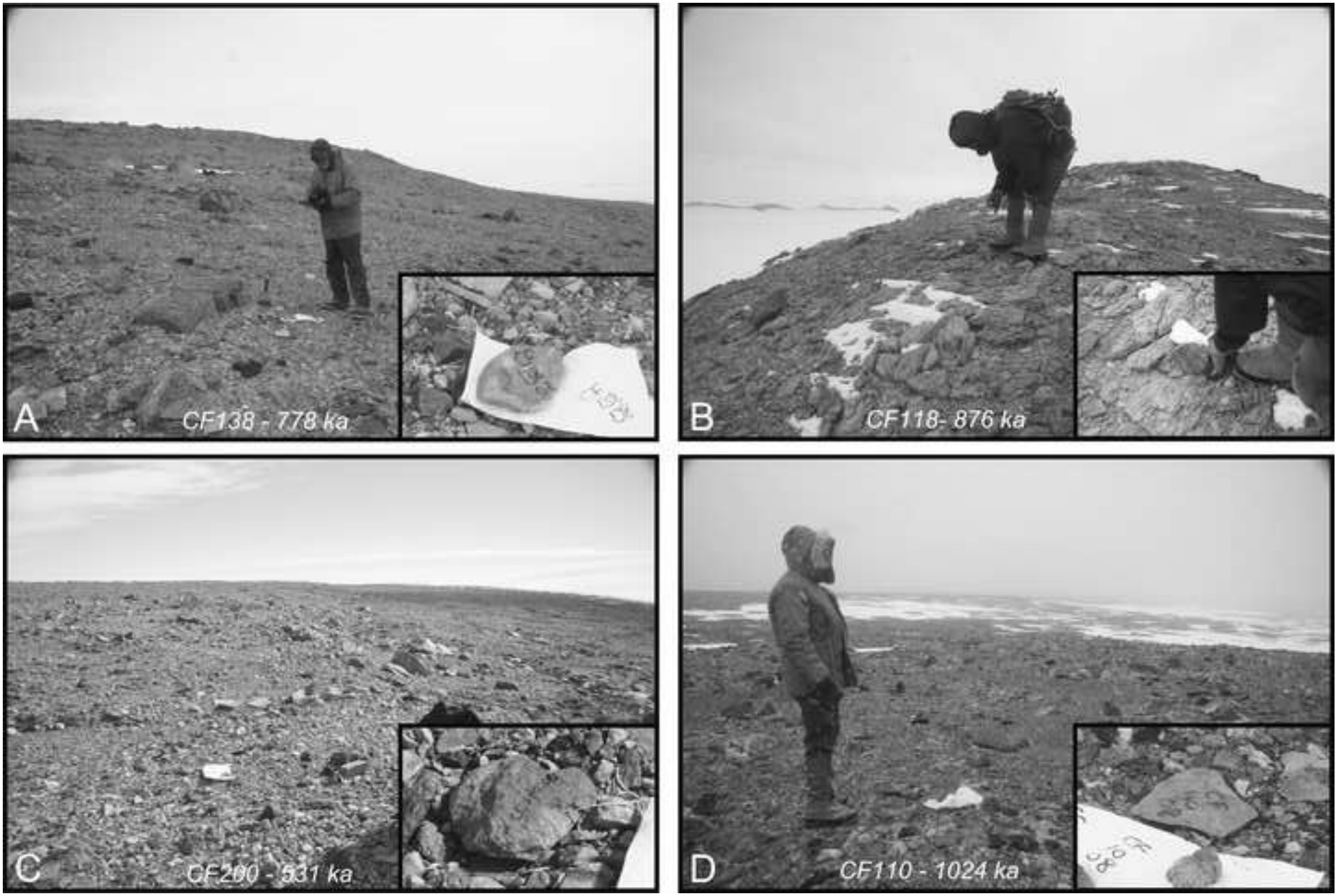

Figure 6 - black and white print version
Click here to download high resolution image

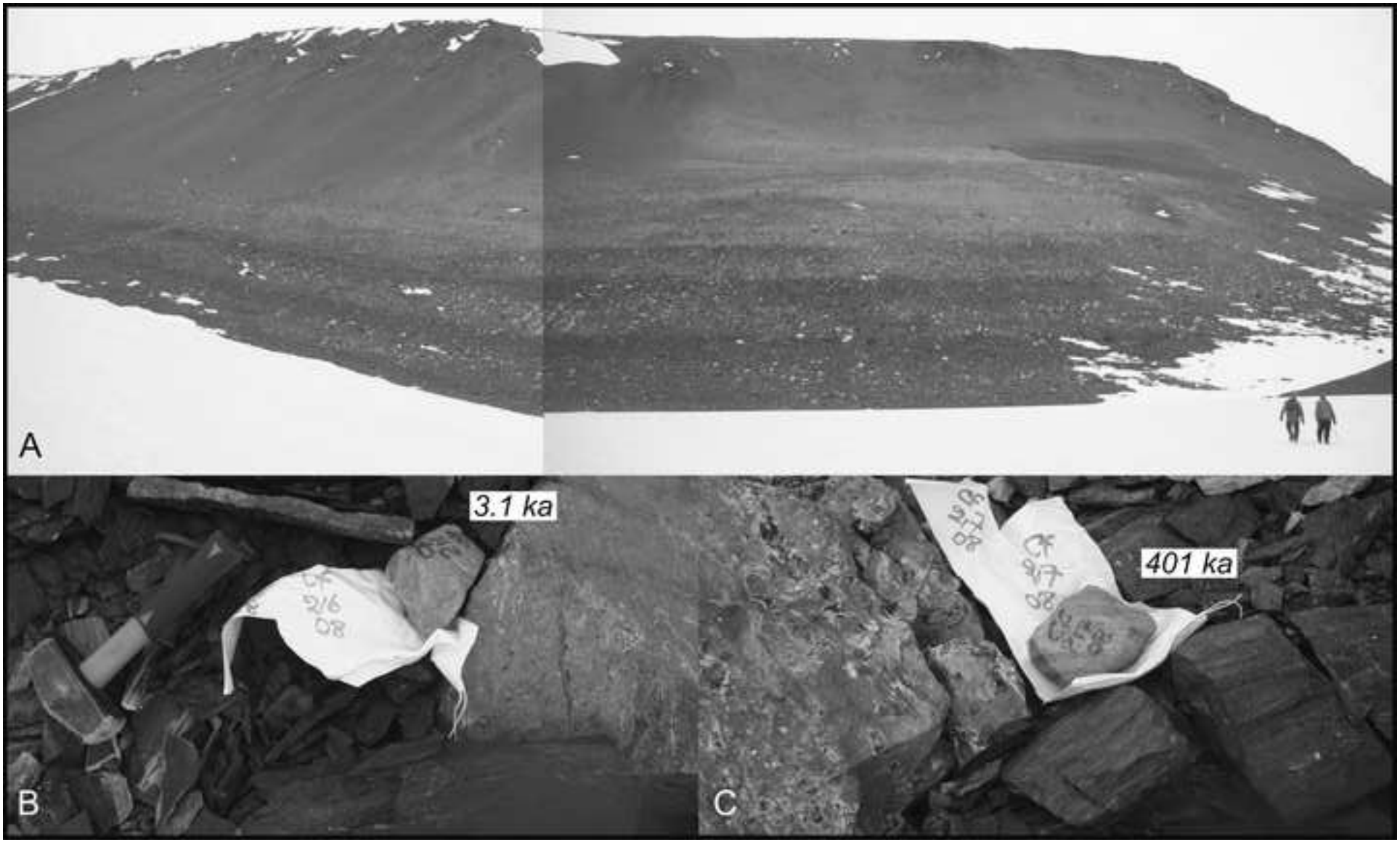

Table 1

Click here to download Table: Hein_Table_1.xls

Table 1

Sample ID	Latitude (dd)	Longitude (dd)	Altitude (m asl)	Lithology	Type*	Thickness (cm)	Shielding correction	Quartz mass (g)	AMS ID†	Nuclide concentration§ ± 1σ (10^6 atom g^{-1} [SiO_2])
Mt Skidmore profile										
CF_118_08	-80.32545	-28.83897	825	Gneiss	E	4.0	0.9992	30.015	b3524	8.374 ± 0.189
									a1017	44.25 ± 1.49
CF_119_08	-80.32545	-28.83897	825	Gneiss	B	5.0	0.9992	30.910	b4512	12.50 ± 0.273
CF_120_08	-80.32436	-28.85522	808	Gneiss	E	4.0	0.9992	30.119	b4509	6.014 ± 0.134
CF_117_08	-80.32098	-28.89879	748	Quartzite	E	3.0	0.9992	28.433	b4497	5.418 ± 0.121
CF_115_08	-80.31669	-28.92190	711	Quartzite	E	4.0	0.9992	34.010	b3528	4.000 ± 0.0882
									a1021	20.69 ± 0.700
CF_70_08	-80.29640	-28.91589	605	Sandstone	E	5.0	0.9954	23.550	b4213	1.488 ± 0.0432
CF_72_08	-80.29640	-28.91589	605	Granite	E	4.5	0.9954	29.003	b3537	1.896 ± 0.0448
									a1030	11.54 ± 0.443
CF_66_08	-80.29664	-28.91595	604	Gneiss	E	5.0	0.9919	29.912	b3540	1.376 ± 0.0333
									a1032	7.761 ± 0.279
CF_64_08	-80.29652	-28.91656	598	Gneiss	E	5.0	0.9919	31.427	b3535	1.976 ± 0.0440
									a1028	12.03 ± 0.476
CF_36_08	-80.29020	-28.67029	576	Quartz	E	3.0	0.9919	31.075	b3833	5.669 ± 0.121
CF_37_08	-80.29020	-28.67029	576	Quartz	E	4.0	0.9919	26.262	b4227	7.461 ± 0.216
CF_78_08	-80.29568	-28.90825	568	Sandstone	E	4.0	0.9954	42.558	b3536	4.984 ± 0.110
									a1029	26.52 ± 0.888
CF_77_08	-80.29567	-28.90827	564	Quartzite	E	5.0	0.9954	29.941	b3748	1.340 ± 0.0340
CF_39_08	-80.28596	-28.68580	508	Granite	E	3.5	0.9919	25.189	b4209	9.820 ± 0.217
CF_40_08	-80.28596	-28.68580	508	Quartz	E	5.0	0.9919	26.938	b4226	5.011 ± 0.150
CF_90_08	-80.29042	-28.84511	495	Sandstone	E	3.5	0.9990	20.923	b3816	2.825 ± 0.0598
CF_91_08	-80.29042	-28.84511	495	Conglomerate	E	5.0	0.9990	28.435	b4208	2.677 ± 0.0830
CF_44_08	-80.28497	-28.68849	474	Quartz	E	3.5	0.9919	31.415	b4225	8.623 ± 0.191
CF_45_08	-80.28497	-28.68849	474	Quartz	E	4.0	0.9919	31.786	b3758	6.475 ± 0.145
CF_95_08	-80.28870	-28.82594	448	Sandstone	E	3.5	0.9989	32.521	b3772	2.594 ± 0.0582
CF_99_08	-80.28009	-28.71314	400	Sandstone	E	5.0	0.9992	30.507	b3771	6.126 ± 0.137
CF_100_08	-80.28009	-28.71314	400	Sandstone	E	5.0	0.9992	31.852	b3541	5.438 ± 0.120
									a1034	29.66 ± 0.997
CF_52_08	-80.27970	-28.70647	399	Sandstone	E	2.0	0.9919	32.871	b3757	8.359 ± 0.187
CF_53_08	-80.27970	-28.70647	399	Sandstone	E	5.0	0.9919	33.235	b3760	4.732 ± 0.106
CF_105_08	-80.27822	-28.71603	382	Quartzite	E	5.0	0.9992	32.421	b3530	7.451 ± 0.164
									a1023	45.61 ± 1.52
CF_104_08	-80.27812	-28.71819	380	Sandstone	E	5.0	0.9992	31.600	b3534	6.200 ± 0.137
									a1025	32.58 ± 1.10
CF_196_08	-80.27249	-28.71008	363	Sandstone	E	5.0	0.9968	25.469	b3529	4.437 ± 0.0984
									a1022	22.80 ± 0.766
CF_108_08	-80.27386	-28.73442	339	Quartz	E	5.0	0.9992	29.075	b3539	3.886 ± 0.0889
									a1031	24.32 ± 0.815
CF_110_08	-80.27386	-28.73442	339	Sandstone	E	3.0	0.9992	29.403	b3770	6.063 ± 0.136
CF_200_08	-80.27017	-28.71768	335	Gneiss	E	3.5	0.9968	22.759	b4221	3.491 ± 0.108
CF_202_08	-80.27017	-28.71768	335	Gneiss	E	3.0	0.9968	19.048	b3821	3.614 ± 0.0794
CF_138B_08	-80.27471	-28.77463	324	Quartzite	E	4.5	0.9997	29.605	b3769	4.749 ± 0.106
CF_139_08	-80.27469	-28.77379	323	Granite	E	4.5	0.9997	27.581	b3751	2.349 ± 0.0526
CF_142_08	-80.27397	-28.77537	309	Sandstone	E	4.0	0.9997	26.553	b3830	3.929 ± 0.0876
CF_143_08	-80.27383	-28.77680	308	Granite	E	4.5	0.9997	25.050	b4224	4.646 ± 0.135
CF_150_08	-80.27216	-28.77998	284	Sandstone	E	5.0	0.9998	34.188	b3759	2.389 ± 0.0536
CF_147_08	-80.27216	-28.77998	284	Sandstone	E	5.0	0.9997	30.776	b3763	3.070 ± 0.0688
CF_155_08	-80.27158	-28.78135	279	Gneiss	E	3.5	0.9998	22.303	b3752	2.232 ± 0.0500
CF_154_08	-80.27147	-28.78090	276	Quartz	E	5.0	0.9998	32.848	b4214	3.346 ± 0.104
CF_56_08	-80.24772	-28.75172	326	Gneiss	E	4.0	0.9919	24.210	b4496	0.8548 ± 0.0208
CF_57_08	-80.26012	-28.85200	278	Granite	E	3.5	0.9919	28.128	b3746	2.307 ± 0.0549
CF_58A_08	-80.26012	-28.85200	278	Gneiss	E	3.5	0.9919	27.906	b3747	0.1911 ± 0.00642
CF_58B_08	-80.26012	-28.85200	278	Gneiss	E	3.5	0.9919	13.410	b4504	0.1868 ± 0.00719
CF_59_08	-80.26188	-28.84317	268	Quartz	E	5.5	0.9919	28.214	b4502	1.240 ± 0.0303
CF_60_08	-80.26188	-28.84317	268	Gneiss	E	5.0	0.9919	26.752	b4500	5.495 ± 0.122

Table 2

Click here to download Table: Hein_Table_2.xls

Table 2

Sample ID	Altitude (m asl)	^{10}Be age* ± 1σ (int)† (ka)	± 1σ (ext)† (ka)	^{26}Al age* ± 1σ (int) (ka)	± 1σ (ext)† (ka)	^{26}Al/^{10}Be ± 1σ
Mt Skidmore profile						
CF_118_08	825	876.4 ± 23.0	131	798.1 ± 36.7	148	5.29 ± 0.21
CF_119_08	825	1526 ± 45.2	273			
CF_120_08	808	598.9 ± 14.5	83.4			
CF_117_08	748	559.9 ± 13.5	77.2			
CF_115_08	711	416.4 ± 9.59	55.3	336.8 ± 12.6	48.8	5.17 ± 0.21
CF_70_08	605	162.6 ± 4.65	20.5			
CF_72_08	605	208.6 ± 4.90	26.3	195.3 ± 7.77	26.6	6.09 ± 0.27
CF_66_08	604	150.5 ± 3.58	18.7	128.3 ± 4.64	16.8	5.64 ± 0.24
CF_64_08	598	221.2 ± 4.91	27.9	207.7 ± 8.56	28.6	6.09 ± 0.28
CF_36_08	576	718.3 ± 17.1	103			
CF_37_08	576	1023 ± 35.5	161			
CF_78_08	568	625.4 ± 15.1	87.7	543.4 ± 22.0	87.7	5.32 ± 0.21
CF_77_08	564	151.7 ± 3.78	18.9			
CF_39_08	508	1637 ± 49.8	303			
CF_40_08	508	681.6 ± 22.5	98.4			
CF_90_08	495	352.8 ± 7.67	46			
CF_91_08	495	337.1 ± 10.7	44.6			
CF_44_08	474	1414 ± 41.1	246			
CF_45_08	474	963.2 ± 25.5	148			
CF_95_08	448	337.5 ± 7.75	43.9			
CF_99_08	400	983.0 ± 26.1	152			
CF_100_08	400	845.3 ± 21.5	126	799.5 ± 36.5	148	5.45 ± 0.22
CF_52_08	399	1474 ± 43.8	260.3			
CF_53_08	399	720.4 ± 18.0	104			
CF_105_08	382	1310 ± 36.9	221	1941 ± 144	713	6.12 ± 0.24
CF_104_08	380	1024 ± 27.1	160	956.7 ± 47.1	194	5.26 ± 0.21
CF_196_08	363	690.5 ± 17.0	98.5	579.5 ± 24.0	95.3	5.14 ± 0.21
CF_108_08	339	605.2 ± 15.1	84.5	651.3 ± 27.8	111	6.26 ± 0.25
CF_110_08	339	1024 ± 27.5	160			
CF_200_08	335	531.0 ± 17.7	73.8			
CF_202_08	335	550.0 ± 13.0	75.6			
CF_138B_08	324	778.4 ± 19.8	114			
CF_139_08	323	347.6 ± 8.00	45.4			
CF_142_08	309	627.8 ± 15.3	88.1			
CF_143_08	308	772.3 ± 25.4	114			
CF_150_08	284	370.5 ± 8.59	48.6			
CF_147_08	284	490.0 ± 11.7	66.4			
CF_155_08	279	341.2 ± 7.86	44.5			
CF_154_08	276	545.9 ± 18.2	76.2			
CF_56_08	326	119.7 ± 2.8	14.8			
CF_57_08	278	357.1 ± 8.77	46.8			
CF_58A_08	278	27.29 ± 0.877	3.36			
CF_58B_08	278	26.7 ± 1.0	3.3			
CF_59_08	268	189.2 ± 4.6	23.8			
CF_60_08	268	1016 ± 30.0	158			
Mt. Sheffield profile						
CF_207_08	474	276.8 ± 6.27	35.5			
CF_204_08	474	734.6 ± 18.2	106			
CF_205_08	474	821.6 ± 19.9	121			
CF_208_08	474	681.3 ± 16.8	97.0			
CF_206_08	474	267.0 ± 8.96	34.9			
CF_209_08	429	199.2 ± 4.36	25.0			
CF_211_08	427	573.6 ± 13.9	79.4			
CF_210_08	427	112.9 ± 3.53	14.2			
CF_212_08	427	849.9 ± 29.4	128			
CF_213A_08	406	135.1 ± 3.02	16.7	171.4 ± 6.02	22.8	8.20 ± 0.34
CF_213B_08	406	172.3 ± 4.1	21.6			
CF_214_08	406	109.3 ± 2.54	13.5	146.7 ± 5.46	19.4	8.72 ± 0.38